Composites: Part A 152 (2022) 106688

Contents lists available at ScienceDirect

Composites Part A

journal homepage: www.elsevier.com/locate/compositesa

Dense and continuous networks of aerial hyphae improve flexibility and shape retention of mycelium composite in the wet state

Tomoko Kuribayashi [a,*], Pauliina Lankinen [b], Sami Hietala [c], Kirsi S. Mikkonen [a,d]

[a] Department of Food and Nutrition, P.O. Box 66, FI-00014, University of Helsinki, Finland
[b] Department of Microbiology, P.O. Box 56, FI-00014, University of Helsinki, Finland
[c] Department of Chemistry, PO Box 55 (A.I. Virtasen Aukio 1), FI-00014, University of Helsinki, Finland
[d] Helsinki Institute of Sustainability Science (HELSUS), P.O. Box 65, FI-00014, University of Helsinki, Finland

ARTICLE INFO

Keywords:
Biocomposite;A
Mechanical properties;B
Electron microscopy;D
Fungal mycelium

ABSTRACT

The mycelium composites composed of fungal mycelium and plant substrate are a practical alternative to petroleum plastic-based foam materials. However, the effects of the physiological traits of fungus on the composites' microscopic structure and mechanical properties remain poorly understood. Here, we compared two basidiomycetes with distinct mycelium morphology and white-decay modes. Cross-sectional observation revealed that the mycelium composites possess a core/shell structure with the shell formed of dense aerial mycelium and the core of plant particles and spongy aerial mycelium. Dense and continuous mycelium networks provided by *Trametes hirsuta* strengthen the mechanical properties of the composite compared to the coarse mycelium networks of *Pleurotus ostreatus*. In particular, the firm mycelial shell skeleton confers high flexibility and shape-retention to the composite in the wet state. This unique characteristic of the mycelium composite indicates its potentials in new industrial applications.

1. Introduction

Fungi, along with plant-based biomass, have drawn industrial and scientific interests as an invaluable renewable natural resource. A wide range of industrial applications on fungi have been proposed and implemented: fungal tissues are used as composite materials and their enzymes are utilized for the modification of biomass [1,2]. A material composed of fungal tissues and plant particles and/or fibers, so-called "mycelium composite", is one of the most practical alternatives to petroleum plastic-based foam materials. In the early 2000s, packaging materials based on mycelium composites were invented by Bayer and McIntyre [3,4]. Since these manufacturing methods of the mycelium composite were reported [5], significant attention not only from industry but also from academic researchers has resulted [6]. To date, further applications and designs of the mycelium composite that have been proposed include apparel [7], buildings [8], acoustic materials [9], vehicle parts [10], and electronic devices [11].

Mycelium composites have mainly been developed for package cushioning and insulation applications in the dry state. In the composite, mycelium is considered to act as a supporting matrix that binds plant particles within its filamentous network structure [12]. Hyphal growth rate and mycelium density have been reported as important factors in the selection of fungal species for the production of mycelium composites [13].

Although several studies have reported morphological and physical properties of mycelium composites [8,9,14,15,16], how the mycelial structures affect the microstructure and mechanical properties of the composites, despite their importance, is poorly understood. In order to optimize the production process and establish an improved design method, it is necessary to understand the actual role of each component within the composite, in particular the effects of the physiological traits of the fungus on the material properties.

While mycelium composites can contain a wide variety of plant substrates from woody and herbaceous plants to agro-waste (grain, millet, etc.) [6,15,17], the fungi used in this class of materials are almost exclusively aerobic basidiomycetes such as *Ganoderma* sp., *Pleurotus* sp., and *Trametes* sp. [6]. Many of these basidiomycetes are also known as white-rot fungi. There are two different modes of plant cell wall degradation implemented by white-rot fungi: selective decay and simultaneous decay [18]. In the former, the fungi decay the cell wall tissue remotely by diffusing low molecular weight substances into the lignified cell wall from the hyphae growing on the lumen. This decay

* Corresponding author.
E-mail address: tomoko.kuribayashi@helsinki.fi (T. Kuribayashi).

https://doi.org/10.1016/j.compositesa.2021.106688
Received 23 July 2021; Accepted 13 October 2021
Available online 20 October 2021

process induces the separation of individual cells at the middle lamella. In the latter, the decay proceeds in the immediate vicinity of hyphae in the lumen, resulting in cell wall thinning. The cell wall decay caused by the hyphal growth can negatively affect the material properties of the mycelium composites. To date, it is unclear if the fungal decomposition of the substrates affects the physical properties of the mycelium composite.

When manufacturing mycelium composites, carbohydrates (e.g. starch) and calcium compounds (e.g. gypsum) are often added as nutrients for fungi, and as pH adjusters for the medium, respectively [5,16]. Tudryn *et al.* reported that adding a carbohydrate at the molding step increases the branch density of the mycelium, which improves the bending strength of the composite [16]. Since the starch and gypsum also function as binders for plant particles [19], it is possible that these additives influence the mechanical properties of mycelium composites. Further understanding of these contributions is beneficial for improving and modifying composites.

This study aims to elucidate the effects of the physiological traits of fungi on the macro- and microstructures and the mechanical properties of the mycelium composite. We compared two fungi that have distinct mycelium morphology and decay modes in terms of the morphology, hydration, and bending properties of the composite. The formation and development of mycelium in the composite can be affected by a combination of the molding dimension and its incubation time. In this study, therefore, we performed analyses using model mycelium composite specimens with small cross-sections (1x1 cm^2) to minimize the effects caused by the structural heterogeneity. Wood was used as the main substrate material because the mechanism of wood decay by white-rot fungi has been better established than with other plant materials [20,21]. To investigate the interplay between fungal growth and substrate decay, extended incubation periods were set after the molding process. We described changes in the macro- to microstructure and mechanical properties of the composites over this long incubation term. Furthermore, we found unexpected flexibility and shape retention ability of the composite in the wet state when the fungi formed a continuous mycelium outer layer. Based on these properties, we further discussed the potentials of the mycelium composites in the wet state use.

2. Materials and methods

2.1. Fungal strains and substrates

Inoculums of Po; *Pleurotus ostreatus* (FBCC0515) and Th; *Trametes hirsuta* (FBCC1239) were obtained from mBRC HAMBI, Finland. Each inoculum was transferred to a 4% malt extract agar plate (9 cm plastic petri dish) and incubated at 27 ± 1 °C until the surface of the agar plate was fully covered by fungal hyphae (Fig. 1). The fungal strains were stored at 5 °C until one day before inoculation on the substrate. For the substrate, a softwood mixture of pine and spruce shaving (Pölkky Oy, Finland), was used as the main component. The median size (D50) of the wood shaving was approximately 2 mm by a sieving method. Its particle size distribution is described in Table S1 and Fig. S1a. As nutrients for fungal growth, oat bran (Raisio oyj, Finland), and coarse wheat flour (Myllyn Paras Oy, Finland) were used. Bulk densities and moisture contents of the wood shaving, oat bran (Fig. S1b), and mixed substrate are summarized in Table S2.

2.2. Preparation of the mycelium composite specimens

Composite specimens were prepared in three steps: preparation of the myceliated substrate (step I), molding and incubating of the composite (step II), and drying and heat treatment (step III). The flow of all processes is illustrated in Fig. S2. Every process between the molding and second incubation except for incubation within the containers, samples have been handled in a laminar flow cabinet. In addition, all tools including metal forms, rubber bands and containers were cleaned and sterilized before being used.

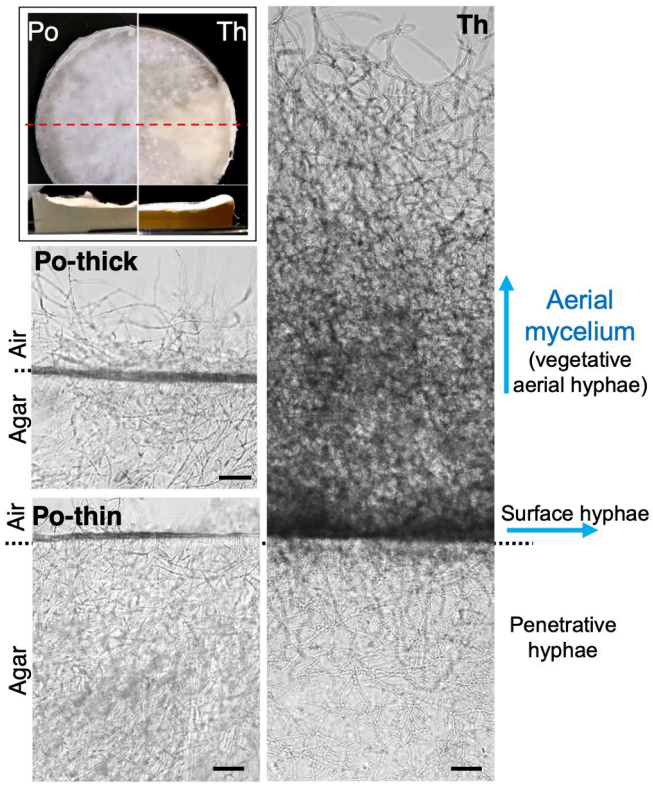

Fig. 1. Mycelium structure on 4% malt extract agar plate (scale bar: 100 μm); left: *Pleurotus ostreatus* (Po); thick (upper) and thin (bottom) part of the mycelium, and right: *Trametes hirsuta* (Th); directions of hyphal extension are indicated by blue arrows. Inset indicates a top view and cross-section of each fungal culture.

2.2.1. Step I: Preparation of the myceliated substrate

270.5 g of air-dried softwood shaving, 67.6 g of oat bran, and 790 ml of deionized water were mixed in a breathable sack (8 L, SacO2, Belgium). The volume of the substrate mixture was estimated at about 2.3 L (Table S2). A total of eight sacks containing this mixture was prepared. The filled sacks were autoclaved at 120 °C for 30 min and cooled to room temperature overnight. Of these, two were used for uninoculated samples as controls. They were processed to step II, after cooling.

One plate of the fungal strain including the agar medium was transferred to each sack. Three replicates were prepared for each fungal species. After the inoculation, the sack was heat-sealed and incubated at 27 ± 1 °C for 27 days (Po) and 24 days (Th) until the substrate was fully covered by the hyphae (Fig. 2a). The pre-incubated substrate, so-called myceliated substrate was kept in the breathable sack and stored at 5 °C until one day before the molding. The myceliated substrate of Po and Th were stored for 23 days and 12 days, respectively at 5 °C.

2.2.2. Step II: Molding and incubation of the composite

10 g of coarse wheat flour (nutrient) was added to one sack of the uninoculated substrate and two sacks of each from Po- and Th-myceliated substrate. The flour and the samples were well mixed by sterilized gloved hands. One sack of the uninoculated substrate and each of the myceliated substrates was set as a flour-free sample. Above processed substrates were molded using hand-made metal forms as illustrated in Fig. 2a. About 13 g of the moist sample (approx. 75 wt% water) was filled in a bottom form (inside dimensions: width 12 mm × height 18.5 mm × length 150 mm), and 11 mm height spacers were set on both edges of the form. Using the upper form, the filled sample was pressed by

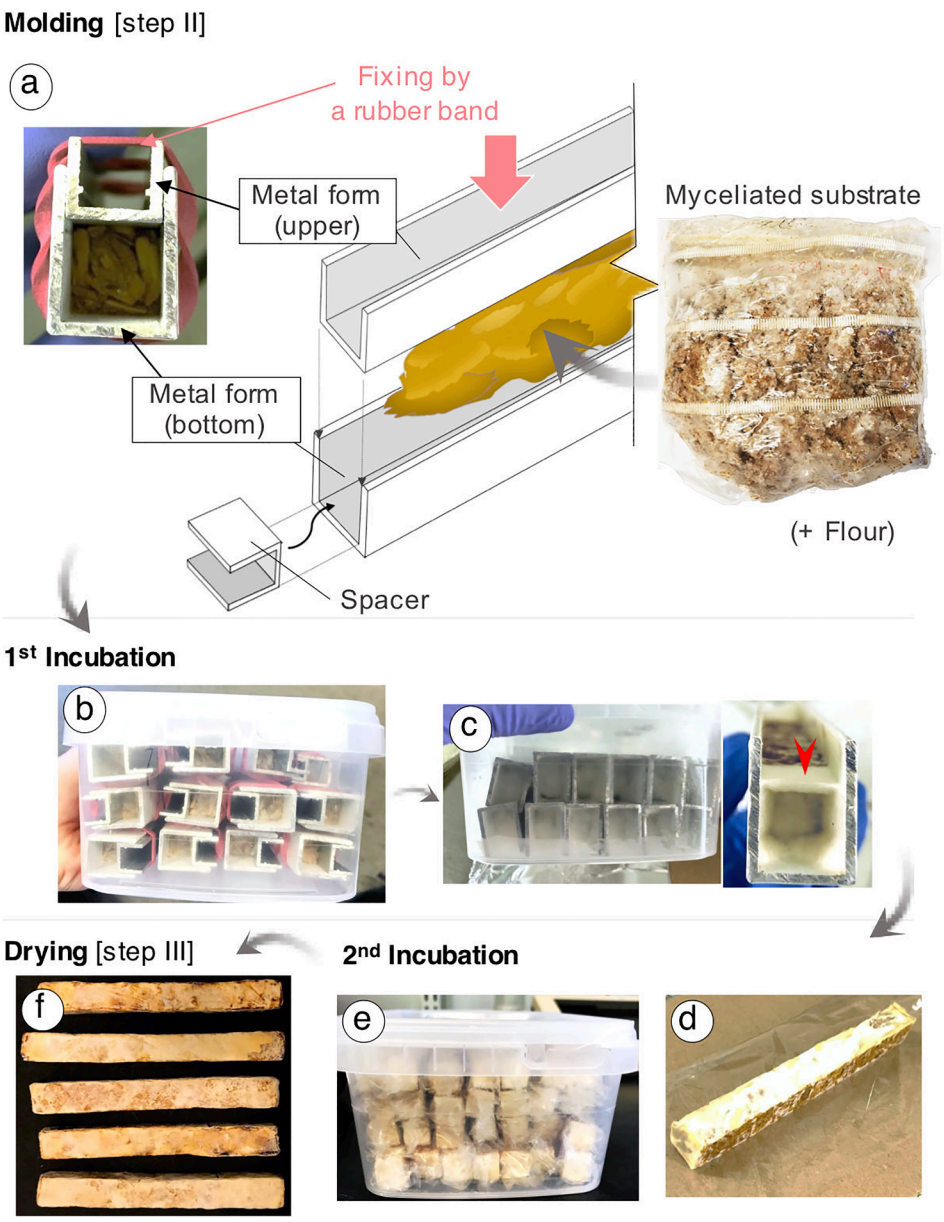

Fig. 2. The molding method and state changing in samples from molding to drying at 27 °C. (a) Scheme of molding method. (b) and (c) Molded samples in a breathable container during the 1st incubation; (b) samples were incubated for 3 days in the fixed forms; (c) left: samples after removing the upper form and a rubber band were incubated for 4 days in the breathable container; right: a sample just after removing the upper form; the red arrow tip points to the mycelium formed at the edge of the sample. (d) Demolded sample on a plastic film. (e) The film wrapped samples in the breathable container during the 2nd incubation; samples were incubated for 1–4 weeks. (f) Th-1w after drying at 27 °C.

the height of the spacers, and the upper form position was fixed by a rubber band (width 4 mm × diameter 80 mm) to keep the sample in the fixation state for three days. To achieve consistent compression conditions in each sample, the number of turns of the rubber band was set to six. By pushing the spacers inward, the sample was adjusted into the intended shape and the spacers were then removed. The intended size and dry density of the molded sample were 11 mm × 11 mm × 100 mm and 0.26 g/cm^3. After the molding, flour-free- and flour-added-uninoculated samples (SO and SOF, respectively), flour-free inoculated samples (Po- and Th- SO), and some of each flour-added inoculated samples (Po- and Th- SOF) were immediately processed to step III. The notation method of each specimen is summarized in Fig. S3.

The remaining flour-added inoculated samples fixed in the forms were incubated in 1.2 L breathable plastic containers (SacO2, Belgium) at 27 ± 1 °C (Fig. 2b). On the third day of the first incubation, the rubber band and upper form were removed (Fig. 2c). After a further four days, the samples were completely demolded (Fig. 2d). Samples processed to step III immediately after the demolding are indicated as Po- and Th-0w. For others, another round of incubation (2nd incubation) was performed. To prevent drying of samples during the incubation, 0.5 ml of sterilized water was added to each sample, and they were loosely wrapped in a plastic film separately. The wrapped samples were packed in the breathable plastic containers and incubated at 27 ± 1 °C for 1, 2, 3, or 4 weeks (Fig. 2e).

2.2.3. *Step III: Drying and heat treatments*

For molded samples of SO, SOF, and Po/Th -SO and -SOF, heat treatment was performed at 90 °C for three hours. Due to the samples not having a set shape, weights (about 42 g/cm^2) were used during heat treatment. Then, only the upper form was removed, and the samples were dried at 40 °C for four days. After drying, the samples were demolded.

During this step for samples performed second incubation (Po/Th −1w, −2w, −3w, and −4w), the plastic film was removed after each incubation period, and the samples were dried at 27 ± 1 °C for three days (Fig. 2f). To limit warpage of the samples during the drying process, a thin and slight weight plastic plate was put on the samples. Pre-dried samples were applied to heat treatment at 60, 90, or 120 °C for three hours. The 0w samples were processed likewise but heat-treated at 90 °C. During the heat treatment, a light metal mesh was put on the samples

to limit warpage caused by heating and drying. The heat treatment was intended to inactivate fungi alongside drying the sample. The hyphal portion was sampled from the heat-treated composite and incubated on a 4% malt extract agar medium for several months. Both fungi were inactivated by heat treatment at 90 °C or higher. Finally, all heat-treated samples were kept at 20 °C, 50%RH until no further weight change was observed. The equilibrium moisture content specimens were subjected to each of the following analyses.

2.3. Moisture content

In this paper, the moisture content (MC) was calculated on a dry basis: dividing the weight of water in the moist specimen by that of the oven-dried specimen (105 °C overnight).

2.4. Morphological observation by scanning electron microscope (SEM)

For the SEM observation, a 3–5 mm thick slice containing the entire cross-section of the specimen was sampled from the middle of the specimen using a razor blade. The samples were observed using a Quanta FEG250 SEM (Thermo Fisher) set at low vacuum mode (40 Pa) and 5 kV accelerating voltage, without any sputter coating.

2.5. Water absorbency

The specimens were immersed in water at room temperature (21 °C). Five replicates were subjected to each condition. A glass plate was placed on the samples to prevent them from floating. The weight of each sample was measured repeatedly from 5 minutes to 48 hours. The weight gain was determined by dividing the difference between wet and dry (20 °C, 50% RH) weight by the dry weight and displayed as %. Before weighing, excess surface water on the samples was removed by wiping with paper towels. The 48 hours water-soaked specimens were immediately subjected to a bending test.

2.6. Three-point bending test

The three-point bending test was applied to dry and wet specimens of five replicates for each set using an Instron model 33R 4465 universal testing machine with a 100 N load cell at 20 °C, 50%RH. The test speed was 3 mm/min using a R4 mm loading nose, and the span length was set as 90 mm. This span length was configured to ensure the span-depth (sample height) ratio to be not less than eight times [22,23]. The amount of head displacement was taken as that of the bending deflection. From the obtained force–deflection curve, the apparent value of flexural secant modulus and maximum flexural stress was calculated using the formulas given in ASTM D7264/D7264M, and the amount of deflection at maximum load was determined. In the flexural modulus calculation, the initial inclination was determined by fitting the force–deflection curve with a linear function in the range x = 0–0.5 mm using gnuplot (www.gnuplot.info). The results of samples with obvious defects such as cracks and voids, as well as corruption during water soaking were excluded from the numerical analysis. The sample was weighed immediately after each test, and its moisture content was measured.

3. Results

3.1. Morphological characterization

3.1.1. Macroscopic structure of the mycelium composite

Two different types of white-rot fungi were used to understand if the decay modes and mycelium morphology affect the resulting composite properties, *Pleurotus ostreatus* (Po) is a selective decay fungus and *Trametes hirsuta* (Th) is a simultaneous decay fungus [24,25]. As shown in Fig. 1, Po forms coarse cotton-like mycelium on the agar plate and it exhibits heterogeneity in thickness. Th forms relatively dense and thick mycelium on the agar plate and the hyphae are tangled. The average hyphal growth rate of Po and Th measured as radial growth [13] was 5 and 7 mm/day, respectively.

Fig. 3a shows a cross-section and top view of the specimens heat-treated at 90 °C. Fungal growth and heat treatment induced discoloration of the substrate and the composite surface. In SO and SOF samples (controls), wood particles could be molded without mycelium thanks to the nutrients acting as glues. The white areas seen in the cross-section and the lateral sides of the incubated samples are mycelia. The visual white tint seen in the myceliated substrate disappeared by the mixing before the molding and was not observed in Po/Th -SO and -SOF. The white color appeared during the first incubation after 2–3 days of molding. During the first incubation, these aerobic fungi resulted in significant hyphal growth on the air-exposed side compared to the sides in contact with the metal forms (Fig. 2c; red arrow and 2d). Po-0w and Th-0w show colonized mycelium inside the specimens, as well (Fig. 3a). After demolding, the mycelia spread over all sides of the samples during the first week of second incubation. The mycelium layer on the surface of the samples became thicker and denser over the course of incubation. In Po specimens, the thickness of the mycelium layer was uneven, and the wood particles were partially visible on the surface even after the four-week incubation (Fig. 3a; white arrow). All the Th specimens were completely covered with the mycelium layer after a week of the incubation (Fig. 2f). The structural features of mycelium in the composite are consistent with those observed on agar plates: a coarse and heterogeneous layer for Po, and a firm, dense and flat layer for Th.

A schematic illustration of the composite cross-section is shown as an inset in Fig. 3a. Inside the mycelium composite, mycelium is randomly distributed around the substrate particles, and the surface of the material is covered with a relatively dense and continuous mycelium layer. A similar structure has been seen in the composites composed of different fungal species and substrates [8,14,15]. The core/shell structure is a common structural feature of this class of mycelium composites. Hyphae that extend in the air are called vegetative aerial hyphae [26]. In this paper, the mycelium formed by the vegetative aerial hyphae is referred to as aerial mycelium (Fig. 1). For clarity, we call the membranous mycelium at the surface “shell mycelium”, and the mycelium inside the composite “core mycelium”.

3.1.2. Changes in the cross-sectional dimension

As shown in Fig. 3b, the dimensions of mycelium composites depend on the incubation period and the fungal species. The height of dry Po- and Th-0w increased due to the springback induced by stress-relieving after demolding as with the controls and Po/Th -SO and -SOF (Fig. 3a). As seen in Po samples before drying, the second incubation process reduced the springback effect (Fig. 3b). No significant change was observed on the dimensions of Po samples during the four-week incubation. The springback also occurred in Th samples, but the extent was smaller than the Po counterparts. The dimensions of Th samples before and after drying were decreased with increasing incubation time.

The moisture content (MC) of samples before drying is shown in Fig. 3b. The initial MC after adding 0.5 ml water at the beginning of the second incubation (Po: 260% and Th: 310%) increased to 350% for Po and 427% for Th after four weeks of incubation. The weight loss value of the moist samples over four-week incubation was 6% for Po and 10% for Th, indicating that Th samples caused a greater degree of wood decay than Po samples. The dimensional shrinkage during the second incubation seen in Th samples before drying was likely caused by mass loss of wood and aggregation effects of hyphal networks. In our sample preparation protocol, no significant compression load was applied to the samples that could cause their deformation, except for the molding. The shrinkage during the heat-drying process was caused by drying.

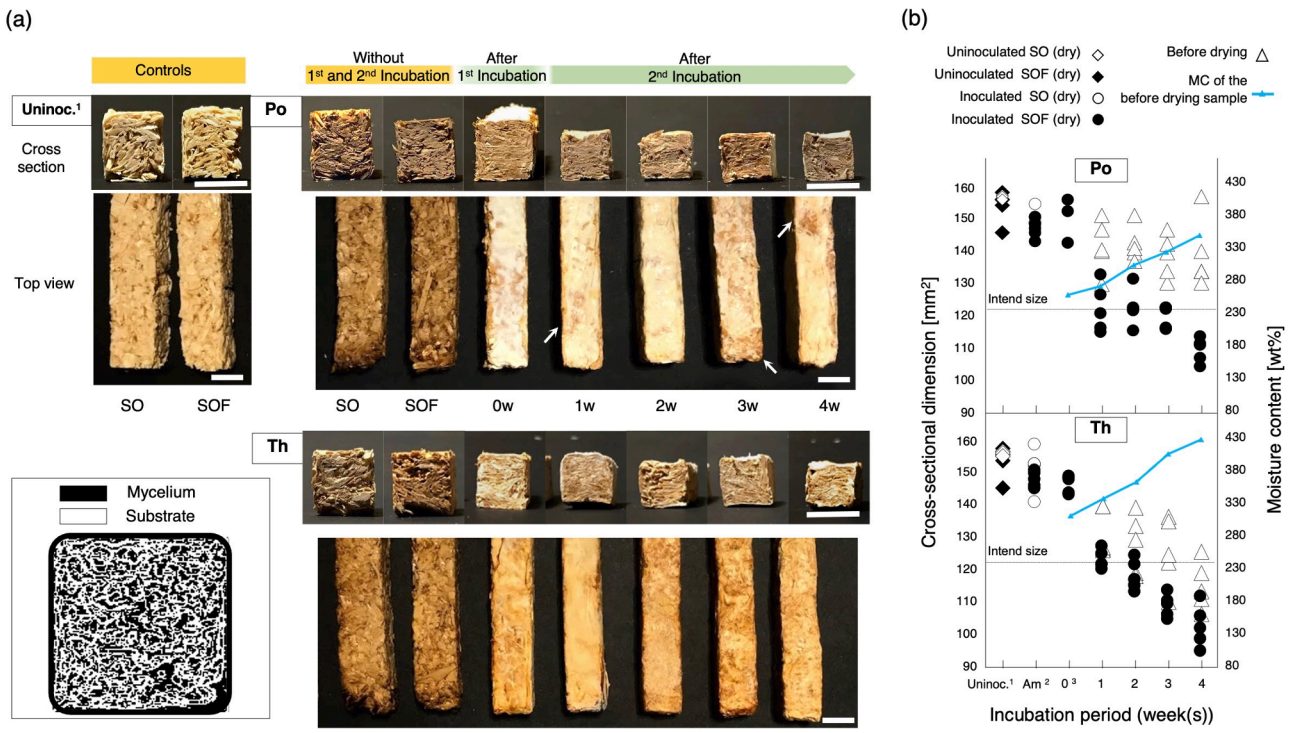

Fig. 3. Morphological changes in mycelium composite for incubation time. (a) Cross-section and top view of the 90 °C treated samples (scale bar: 10 mm); inset is a schematic illustration of a cross-section of the mycelium composite. (b) Cross-sectional dimension of the samples; all indicated dried samples were heat treated at 90 °C for 3 h; moisture content (MC) of the before drying samples was plotted in the second y axis. *Note.* [1]Uninoc. = uninoculated (controls); [2]Am = after molding (without processing of 1st and 2nd incubation); [3]0 = after 1st incubation.

3.1.3. *Cross-sectional observation by SEM*

In the composite, the wood particles are randomly distributed. In SOF, many gaps up to a millimeter in size were visible between the particles (Fig. 4a). Glue-like layers with no cell or fibrous structure were observed between and on the surface of wood particles (Fig. S4). They were most likely the nutrient additives transformed from the initial granular shape into these layered structures through hydration, heating, and drying processes. In some sections, the layers bonded the wood particles as indicated by white arrow tips in Fig. 4b and c. In Po-and Th-SOF, the surface of wood particles was covered with mycelium and/or nutrients layers, but the gaps between the wood particles remained open (Fig. 4b-e, and S5). Hyphae were attached to the wood cell wall lumen as indicated by the blue arrow tip in Fig. 4c, in both Po and Th samples. No noticeable difference was found in the state of hyphae on the lumen after four weeks of second incubation.

After the four weeks of incubation, gaps between the wood particles were filled with mycelium (Fig. 4f and g). In Po-4w, cracks between the wood particle and core mycelium were likely induced by the sectioning (Fig. 4f; yellow arrow). The Po specimens were more fragile than the Th specimens, which caused challenges in preparing sections with a thickness of 3 mm or less. The core mycelium possessed a sponge-like texture, and Po showed a coarser structure than Th (Fig. 4f-i). Drying shrinkage of hyphae was observed in the core mycelium of Po and Th, as also seen in other species [27]. Hyphae lost their tuber structure and became flattened and aggregated with adjacent hyphae (Fig. S6). At the interface between core mycelium and wood particles, a scaffold-like structure composed of hyphae and/or nutrients was formed, and the hyphae grew from them towards the gaps between wood particles (Fig. 4j and k; blue arrow tips). Excess water was not observed at the molding, and the saturated MC of the wood particle is above 440% (Table S2). Thus, the hyphae observed in the core mycelium growing in the empty spaces between the wood particles are vegetative aerial hyphae. The hyphae on the lumen and in the tracheids possibly grew in the wet phase.

The outermost surfaces of Po-4w and Th-4w were covered by a continuous shell mycelium. The Th shell mycelium was smoother than Po (Fig. 4g and f; red arrow tips). Fig. 4h and i show the maximum thickness of shell mycelium found in the Po-4w and Th-4w sections, respectively. The shell mycelium is composed of a thin layer at the outermost surface and spongy mycelium beneath. As detailed by Santos *et al.*, the outermost surface of the composite has a planar structure formed by binding hyphae oriented in-plane [15]. The aerial hyphae that extend horizontally on the solid medium are known as surface hyphae and stolon (Fig. 1) [27], but the planar hyphal structure on the composite surface is formed at the tip of the vegetative aerial hyphae and differs from those (Fig. 4h and i). The wrapping film used in the second incubation may have worked as a guide for parallel hyphal orientation. Slight compression during the drying likely affected the surface structure of shell mycelium. In either case, the continuous planar structure might be advantageous for the mechanical properties of the composite. Further investigation will be made in a separate study to elucidate the formation of this planar hyphal structure produced during the second incubation and drying.

In the Th-4w, cracking and thinning of the wood cell wall and partial detachment of the cell wall from the middle lamella were observed more clearly than in Th-SOF (Fig. S7). In this observation, the nutrients layers remained even after four weeks of incubation in both Po and Th specimens (Fig. S8).

3.2. *Physical properties*

3.2.1. *Water absorbency*

The uninoculated samples collapsed when a minimal force was applied after being soaked in water for about five minutes. Meanwhile, most samples with mycelium formation maintained their shape during the 48-hour soaking. Aerial hyphae have a hydrophobic surface covered with self-assembling proteins called hydrophobins [28]. Water contact angles were reported above 100° for purified hydrophobin coatings and

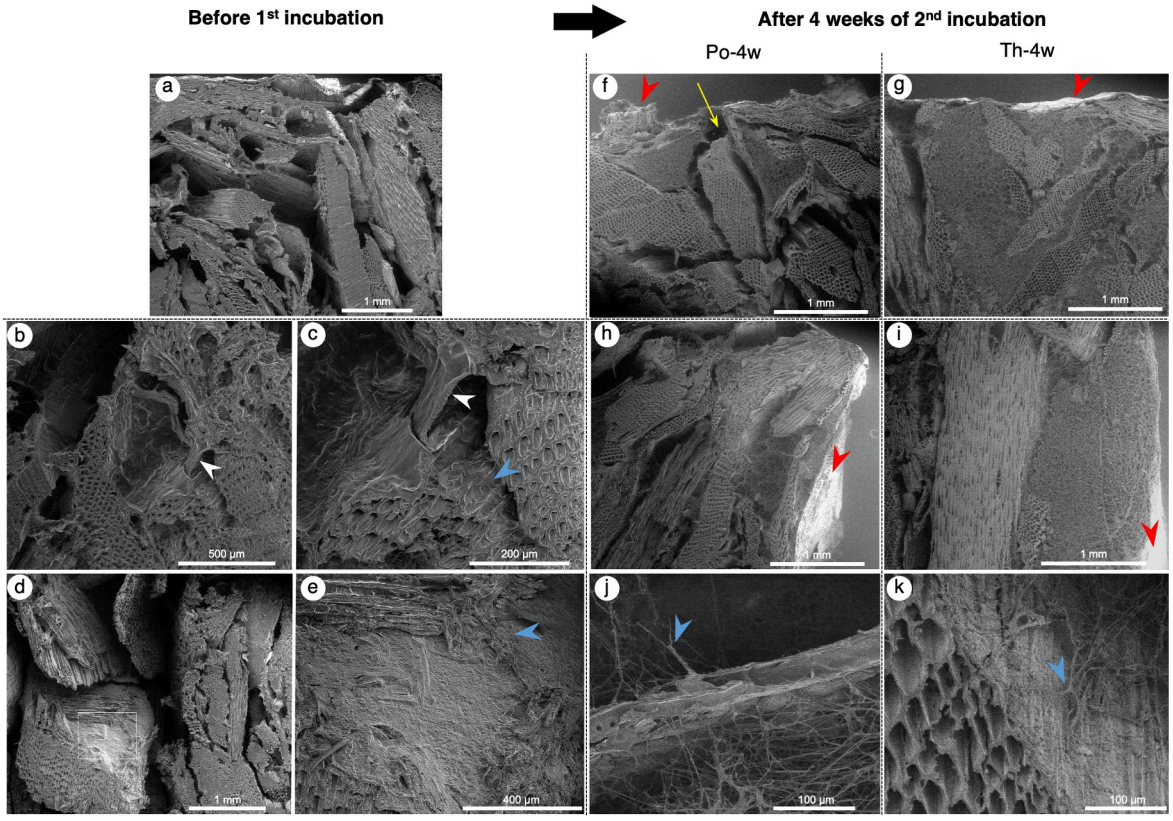

Fig. 4. State of the mycelium composite cross-section by SEM observation. (a)-(e) Samples without incubation; (a) SOF; (b) and (c) Po-SOF; (d) and (e) Th-SOF; (c) and (e) detail a higher magnification view of (b) and (d), respectively. (f)-(k) Samples after 4 weeks of 2nd incubation; (f), (h), and (j) Po-4w; (g), (i), and (k) Th-4w; (h) and (i) show the edge of each sample, focused on the thickest shell mycelium in the section; (j) and (k) high magnification view of the interface area between core mycelium and wood particle of each sample. *Note.* Arrow tips of white = layers formed by nutrients, blue = hyphae, and red = surface layer of the shell mycelium; yellow arrow points to a crack between wood particles and the core mycelium.

pure mycelium sheets [28,29]. The shell mycelium of the composite showed a temporal water repellency (Fig. S9). Due to the surface roughness of the composites, the apparent contact angle was lower (<90°) than the reported values. Water was absorbed into the composite in a few minutes, and the shell mycelium became slightly translucent, likewise in pure mycelium sheets reported by Sun *et al.* [29].

During the water soaking, water penetrated the composite through gaps in the shell mycelium. Visual observation of the cross-section of wet

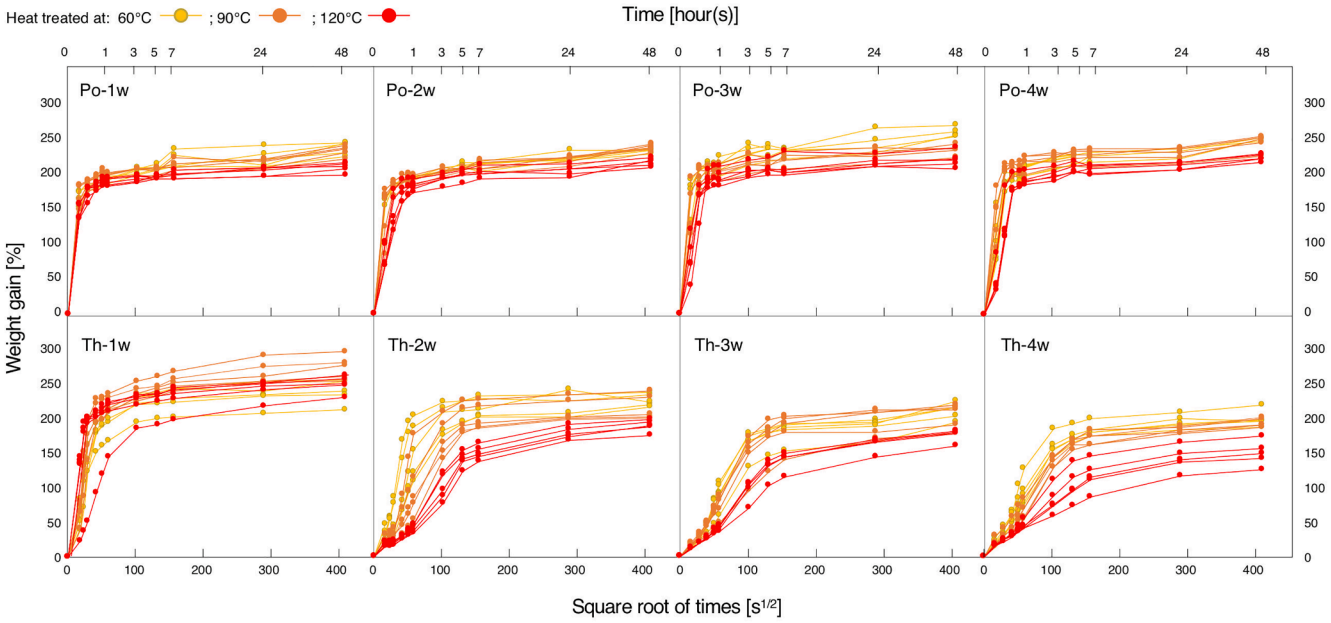

Fig. 5. Weight gain (%) of the samples over water soaking for 48 h.

samples after the bending test confirmed the water reached the center core of the composite in all samples. The moisture content values of the samples after water soaking were above 200% and the color changes in the wood and mycelium wet suggested that water penetrated in the wood and the hyphal networks. Hyphal cell walls also presumably absorbed water [27]. Due to the porosity of the composite, the macroscopic dimension did not significantly increase (Table S3).

Weight gain of samples as a function of the soaking time is shown in Fig. 5. Note that the weight and moisture content of the initial samples differ with fungal species and sample conditions. The measured weight and moisture content at 20 °C, 50%RH are summarized in Tables S4 and S5, respectively. The weight gain of the Po samples was about 200% after one hour of soaking, and a total of five samples collapsed during the test regardless of the heat treatment temperature and the incubation period (Fig. 5). The wet moisture content (MC) of Po samples was in the range of 260–337%, and higher heat treatment temperature resulted in slightly lower MC, but the MC values were almost equal or higher than wet MC of SO (297%) (Table S6). A coarse mycelium of Po acts as a retardant against water penetration, but the water absorbency of the composite corresponds mostly to that of the substrate. In the Th samples subjected to long incubation (>2 weeks), the saturated water absorption decreased as low as 120%, and the absorbing speed became significantly slow as the incubation period and heat treatment temperature increased. The wettability of wood does not change by heat treatment below 130 °C [30]. Thus, decreasing water absorbency resulted from the mycelium formation and physicochemical modification of the mycelium upon heat treatment.

3.2.2. *Bending properties*

In the bending test, samples without visible defects fractured at the bottom center of the sample in the dry and wet states. Indentation by the loading nose was not observed. Fig. 6 shows typical force–deflection curves. The shapes of the curves were significantly different between the dry and the wet state. The dry samples showed a brittle fracture between wood particles, regardless of fungal species. The strength of the wet sample was reduced to about one-tenth compared to the dry samples, and the amount of deflection until fracture became larger. From microscopic aspects, as pointed out by arrows, the curve showed the generation of microcracks in the vicinity of 0.2 mm and 1.0 mm of the deflection (Fig. 6; left inset). Such microscopic fracture formation has been proposed based on contrast the finite-element simulation with the experimental value under compression load of a mycelium composite [12]. Interestingly, in the wet samples, the discontinuous behavior above was not observed, and the initial linear region extend (Fig. 6; right inset).

To investigate changes in the strength properties provided by differences in the sample preparation conditions, we used the apparent values of flexural modulus (F) and maximum stress (σ_{max}) for comparison. All values of the flexural parameters are summarized in Tables S5 and S6. In a dry state, σ_{max} and deflection at maximum load (δ_{max}) of the composite samples did not show a significant difference depending on the fungal species, incubation time, and the heat treatment temperature. The average value of the σ_{max} was distributed in the range of about 630–940 kPa, and the variation due to sample preparation conditions was within sample variability (Table S5). Thus, we focused on the value of F, which has a relatively small variability between the samples. We investigated a relationship between density and F to consider the effects of wood decay and the formation of mycelium structures. Incubated Po samples have a density distribution of 0.24–0.29 g/cm^3, and the higher the density, the larger F became (Fig. 7a; left). The density of Th samples was lower than that of Po samples (0.22–0.26 g/cm^3), but F was roughly the same. In the Th series no correlation was observed between incubation period and the density (Fig. 7a; left).

F and σ_{max} of Po- and Th-SO samples are remarkably lower than incubated samples, (Fig. 7a; right, and Table S5), which indicated that the mycelium formed during pre-incubation has a minor contribution to the flexural strength of the composite. Thus, the formation of mycelial core/shell skeleton is necessary to develop the strength of the composite.

F increased with the addition of flour regardless of the presence of mycelium (Fig. 7a, right). Po-SOF had a higher F than SOF, while Th-SOF had a lower F. This difference might be due to the differences in the interface state between the flour and the wood particles. Since the hydrophobicity of the surface of the substrate becomes higher with the formation of aerial mycelium, the wettability of hydrated flour on the myceliated substrate becomes lower. The mycelium formation of Th was more advanced on the substrate than that of Po, so the Th mycelium might prevent flour from adhering to the substrate surface.

In a wet state, the δ_{max} was significantly larger for the Th samples than the Po samples (Fig. 7b). Some of the Th samples incubated for longer than three weeks did not break at a displacement of 25 mm (Table S6). For samples of both fungi, the higher F and σ_{max} were obtained with higher heat treatment temperature. The lower stiffness of the composite in the wet state results from the enhanced stretchability of mycelium caused by the hydration. Under the center concentrated load of bending, the tensile stress is generated at the bottom of the sample. In the wet Th samples, visible cracks were not observed at their lower side, in which indicated the bottom shell mycelium layer stretched and followed the deformation. The firmness and thickness of shell mycelium

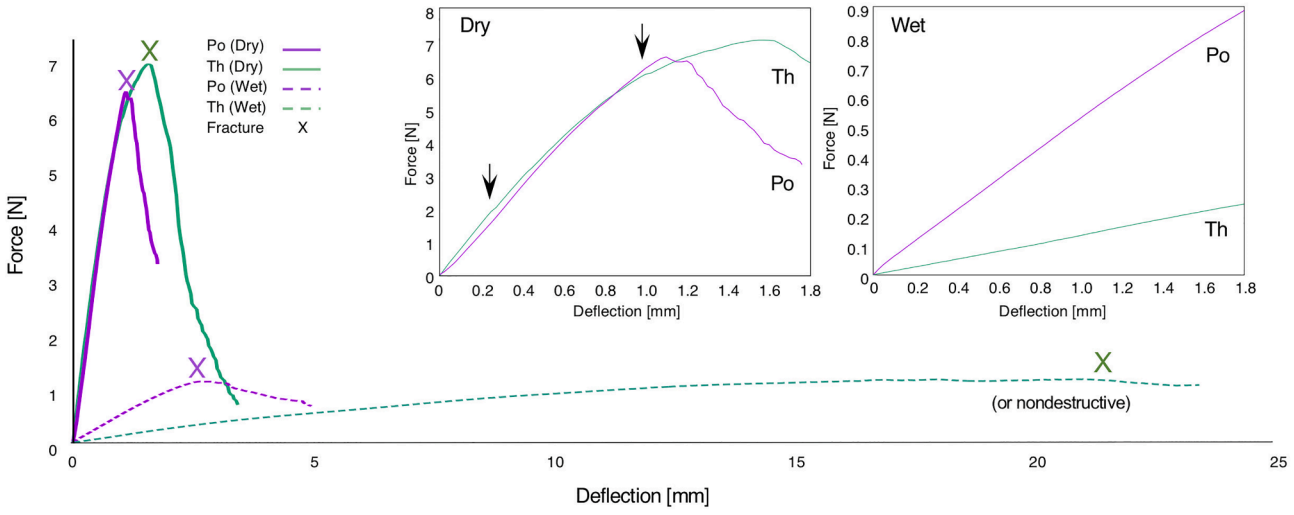

Fig. 6. Typical force–deflection curves of Po and Th samples; insets are enlarged views of the deflection region (≤1.8 mm) of dry state (left) and wet state (right).

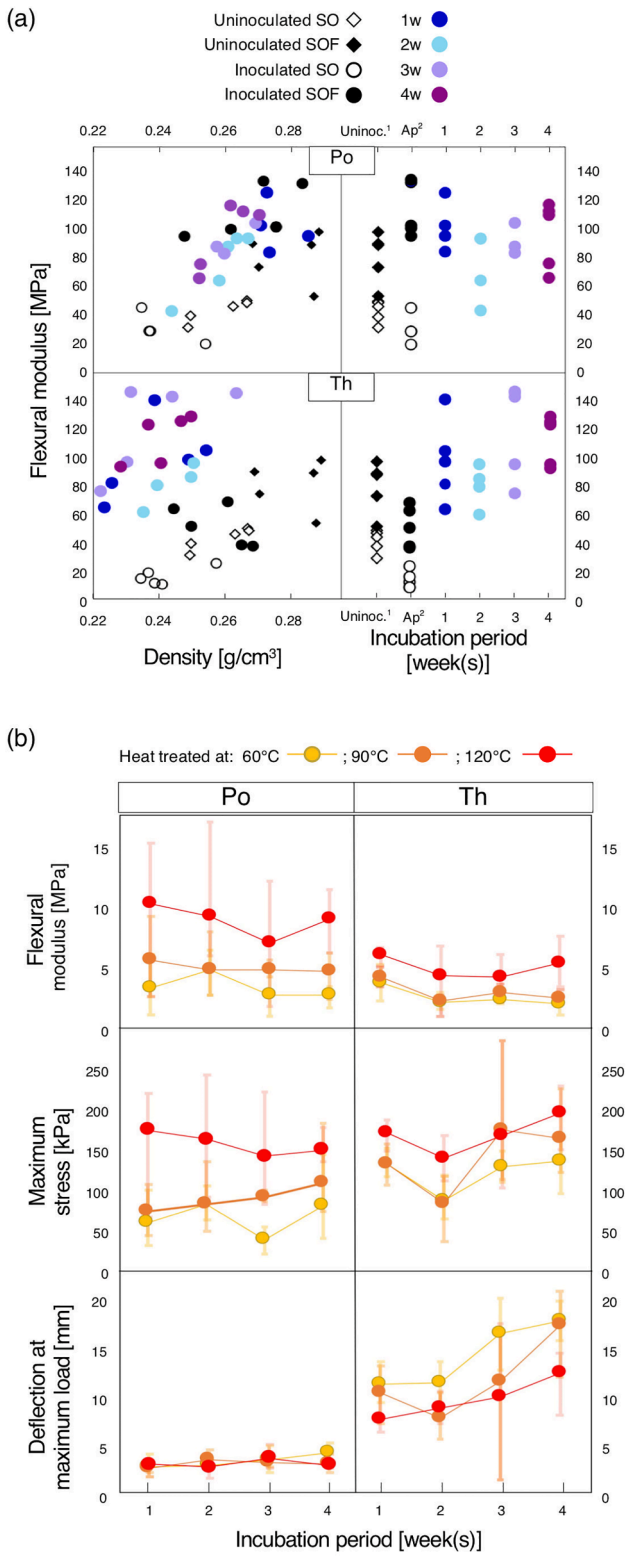

Fig. 7. Flexural parameters of dry and wet states. (a) Flexural modulus of dry Po and Th samples plotted against density (left) and incubation period (right); 90 °C heat treated samples results were indicated. (b) Flexural modulus, maximum stress, and deflection at the maximum load of wet Po and Th samples plotted against incubation period. *Note.* [1]Uninoc. = uninoculated; [2]Ap = after pre-cultivation (Po/Th –SO and SOF).

are crucial to confer flexibility to the mycelium composite.

4. Discussions

4.1. The morphogenetic mechanism of mycelium composite and decay on the wood substrate

As illustrated by Tudryn *et al.*, hyphae are crushed and dispersed by the mixing at the molding step [16]. Each hypha serves as a fungal growth starting point and eventually covers the entire molded materials. Over the incubation period, wood decay was certainly progressed. To estimate the degree of wood decomposition and hyphal growth, we attempted chemical analysis by ATR-FTIR and solid-state ^{13}C CP/MAS NMR (Figs. S10, S11, and Table S7 (IR); Figs. S12 and S13 (NMR)). Both of their spectra of the mycelium composites contained many overlapping lines, making it difficult to gain quantitative information. In the IR and NMR spectra, characteristics of pure mycelium appeared on the spectrum after one week of second incubation, and their contribution increased with incubation time. The ratio of fungal tissue in the composite increased more during the processes of second incubation than during the pre-incubation, and a longer incubation causes a higher increase. The results are rational as the vegetative aerial hyphae are the majority in the core and shell.

The hyphal growth in aerobic fungi above solid medium, as well as the role of the aerial hyphae, have been discussed in literature. Rahardjo *et al.* investigated the role of the aerial hyphae using *Aspergillus oryzae* in terms of solid-state fermentation [31]. They stated that the vegetative aerial hyphae, not like surface hyphae, mainly contribute to oxygen uptake, and the concentration of the aerial mycelium is a limiting factor for the respiration rate. As simulated by Sugai-Guérios *et al.* [26], vegetative aerial hyphae stop growing when they enter congested spaces, resulting in an upper limit to the local biomass concentration. The concentration of the vegetative aerial hyphae is one of the important parameters to control the formation of mycelial skeletons in the composite. In the mycelium composite, hyphae in shell mycelium facing an aerobic environment grow relatively fast during the incubation after demolding compared to the hyphae in core mycelium. The forming of the shell mycelium reduces oxygen supply into the core of the composite, which may slow down hyphal growth of core mycelium. To promote the growth of hyphae in the composite, methods like extending the incubation time, controlling oxygen concentration in the solid medium, and mixing growth accelerators have been suggested [14,15]. In cases where the formation of core mycelium stops due to saturation, extending the incubation period is not an efficient solution to facilitate mycelial skeleton formation. A forced feed of humid oxygen into the composite very likely expedites the growth of the core and shell mycelium, even though the effects on the concentration limit of the core mycelium still need to be investigated. Although it was difficult to quantify the hyphal growth and wood degradation of the composites in this study, the forced promotion of hyphal growth rate would hasten the substrate decay. The decay of the main substrate contributes lightweighting of the composite, while it causes dimensional shrinkage on the composite, as shown in the long-incubated Th samples (Fig. 3b). To reduce substrate decay, it is necessary to optimize the ratio of nutrients added to the substrate.

4.2. Contributions of mycelium to composite mechanical properties in a dry state

In the mycelium composite, core mycelium is sparse and discontinuously connects wood particles (Fig. 4h and g). Shell mycelium surrounding the material allows the composite to hold a solid shape. Applying a cutting force to composite specimens compromised the integrity of shell mycelium and induced the crumbling between wood particles from the cut section. This effect was more pronounced in Po composite with underdeveloped mycelial skeletons. Thus, the firm and

continuous mycelial shell structure is key to control the shape stability of the composite. For an effective fungal species selection, attention should be given to the morphological features of the aerial mycelium above the agar medium, in addition to the reported hyphal growth rate and density [13].

Dense and continuous mycelium structures reinforce mycelium composites. However, the reinforcing mechanism in mycelium composite greatly differs from that in general wood particle composites. For instance, in particleboard manufacturing, resins harder than wood are broadly used as an adhesive. The cured resin forms a continuous matrix in the material and binds the wood particles. In the mycelium composite, hyphal networks aggregate wood particles by filling in the gap between them, and the residue of nutrients supports the aggregation. As considered in the literature, secreted proteins of the fungus and the degraded wood components are likely to be involved in the agglomerate [32]. Those agglomerate agents contribute to the strength of the composite, but they are more fragile than wood particles. The cracks generated at the initial flexural deformation in a dry state most likely occurred in the region of those agglomerate agents. In fact, the strength of these mycelium composites is about one-thousandth of those of the above-mentioned wood boards, being more akin to the range of the strength of a biscuit, for instance [33]. Thus, simple molded mycelium composites are in general suitable for applications such as filling materials taking advantage of their porosity and lightweight rather than load-bearing applications. To use the composite as a structural element, it is necessary to improve strength by consolidation and hybrid structuring [14,34].

4.3. Hydration effects and applications in the mycelium composite

The difference in mycelial firmness appears noticeable when wet. A composite produced by coarse mycelium has low water resistance. In contrast, firm mycelium improves shape-retention and flexibility in a wet state composite. The degree of hydration can be controlled by the heat treatment temperature. Previously, the rapid water absorption of mycelium composites has been regarded as a problem in the practical uses [34]. This unique characteristic found in the Th composite changes the typical drawback of the composite to a potential advantage. Its high-water absorbency as a composite, shape retainability provided by shell mycelium, water-retention of plant substrate, and biodegradability offer new potential industrial applications of the mycelium composite in a wet state use. For instance, seedling-raising containers for agronomic crop production are likely feasible as demonstrated in the preliminary results in SI (Fig. S14). Influences for the seedling growing environment (e.g. pH, drainage, and contamination resistance against plant pathogenic microbe) should be considered to optimize the manufacturing process including secondary treatment. In this composite, the plant substrate has been partially degraded by fungus, thus it would give benefit the acceleration of biodegradation after the use.

5. Conclusion

Mycelium composites possess a core/shell structure with the shell formed of dense mycelium, and the core of plant particles and spongy mycelium. Both core and shell mycelial skeletons were vegetative aerial hyphae. The structural feature of the aerial mycelium on the agar plate corresponds well to the shell mycelium morphology of the composites. The firm mycelial structure provides a greater sealing effect between wood particles than the coarse mycelial structure.

The structure of mycelium more significantly affects the physical characteristics of the mycelium composites than fungal decay modes. In a dry state, mycelium and nutrients develop the mechanical strength of the mycelium composite. In a wet state, differences in firmness of the mycelium structure clearly appear on the flexural properties. Dense and continuous shell mycelium structure imparts flexibility to the composite and improves shape retention of the composite in water. The heat treatment temperature affects the water absorbency and the flexural strength in a wet state of the composite. Although further investigation is required to understand if the mechanical properties of the mycelium composites of Th is unique to this species, the exceptional properties of its hydrated mycelium offer new potential industrial applications. These findings brought by the physiological traits of fungus will pave the way to establishing an improved design method for the mycelium composites.

Declaration of Competing Interest

The authors declare that they have no known competing financial interests or personal relationships that could have appeared to influence the work reported in this paper.

Acknowledgements

This work was supported by the Academy of Finland (project numbers:311244, 314244, and 335689). This study has greatly benefited from The mBRC HAMBI, part of the Biodiversity Collections Research Infrastructure (HUBCRI) in the Helsinki Institute of Life Science, University of Helsinki, Finland for providing fungal strains, and Electron Microscopy Unit of the Institute of Biotechnology, University of Helsinki, Finland for providing laboratory facilities. We want to thank our laboratory colleagues, Tuovi Mustakanges, Jutta Varis, and Mikko Kangas of the Department of Food and Nutrition for their technical supports. We express our special thanks for the tolerant support provided their equipment of Dr. Taina Lundell and Eero Kiviniemi of the Department of Microbiology, University of Helsinki. Additionally, we are grateful to Troy Faithfull of the Department of Food and Nutrition, University of Helsinki for critical reading of the manuscript. We wish to thank Dr. Yu Ogawa of CERMEV-CNRS, France for practical advice in the application of SEM.

Appendix A. Supplementary data

Supplementary data to this article can be found online at https://doi.org/10.1016/j.compositesa.2021.106688.

References

[1] Cerimi K, Akkaya KC, Pohl C, Schmidt B, Neubauer P. Fungi as source for new bio-based materials: A patent review. Fungal Biol. Biotechnol 2019;6(17).
[2] Meyer V, Basenko EY, Benz JP, Braus GH, Caddick MX, Csukai M, et al. Growing a circular economy with fungal biotechnology: A white paper. Fungal Biol. Biotechnol 2020;7(5).
[3] Zeller P, Zocher D. Ecovative's breakthrough biomaterials: Fungi 2012;5(1):51–6.
[4] Bayer E, McIntyre G, Method for producing grown materials and products made thereby. US009485917B2; Nov. 8, 2016.
[5] Holt GA, McIntyre G, Flagg D, Bayer E, Wanjura JD, Pelletier MG. Fungal mycelium and cotton plant materials in the manufacture of biodegradable molded packaging material: Evaluation study of select blends of cotton byproducts. J. Biobased Mater Bioenergy 2012;6:431–9.
[6] Attias N, Danai O, Abitbol T, Tarazi E, Ezov N, Pereman I, et al. Mycelium bio-composites in industrial design and architecture: Comparative review and experimental analysis. J Clean Prod 2020;246.
[7] Jiang L, Walczyk D, McIntyre G. A New Approach to Manufacturing Biocomposite Sandwich Structures: Investigation of Preform Shell Behavior. J Manuf Sci Eng 2017;139(2):021014.
[8] Elsacker E, Vandelook S, Brancart J, Peeters E, De Laet L. Mechanical, physical and chemical characterisation of mycelium-based composites with different types of lignocellulosic substrates. PLoS ONE 2019;14.
[9] Pelletier MG, Holt GA, Wanjura JD, Bayer E, McIntyre G. An evaluation study of mycelium based acoustic absorbers grown on agricultural by-product substrates. Ind Crops Prod 2013;51:480–5.
[10] Kalisz RE, Rocco CA. Method of making formed mycelium structure. Foamed mycelium structure and method. US008227233B2; Jul. 24, 2012.
[11] Vasquez ES, Vega K. From plastic to biomaterials: prototyping DIY electronics with mycelium. In: Adjunct proceedings of the 2019 ACM international joint conference on pervasive and ubiquitous computing and proceedings of the 2019 ACM international symposium on wearable computers (UbiComp/ISWC '19 adjunct). New York, NY, USA: Association for Computing Machinery; 2019. p. 308–11. https://doi.org/10.1145/3341162.3343808.

[12] Islam MR, Tudryn G, Bucinell R, Schadler L, Picu RC. Mechanical behavior of mycelium-based particulate composites. J Mater Sci 2018;53:16371–82.
[13] Jones M, Huynh T, John S. Inherent species characteristic influence and growth performance assessment for mycelium composite applications. Adv Mater Lett 2018;9:71–80.
[14] Appels FVW, Camere S, Montalti M, Karana E, Jansen KMB, Dijksterhuis J, et al. Fabrication factors influencing mechanical, moisture- and water-related properties of mycelium-based composites. Mater Des 2019;161:64–71.
[15] Santos IS, Nascimento BL, Marino RH, Sussuchi EM, Matos MP, Griza S. Influence of drying heat treatments on the mechanical behavior and physico-chemical properties of mycelial biocomposite. Compos Part B Eng 2021;217:108870.
[16] Tudryn GJ, Smith LC, Freitag J, Bucinell R, Schadler LS. Processing and morphology impacts on mechanical properties of fungal based biopolymer composites. J Polym Environ 2018;26:1473–83.
[17] Tacer-Caba Z, Varis JJ, Lankinen P, Mikkonen KS. Comparison of novel fungal mycelia strains and sustainable growth substrates to produce humidity-resistant biocomposites. Mater Des 2020;192:108728.
[18] Schwarze FWMR. Wood decay under the microscope. Fungal Biol Rev 2007;21:133–70.
[19] Bumanis G, Vitola L, Pundiene I, Sinka M, Bajare D. Gypsum, geopolymers, and starch-alternative binders for bio-based building materials: a review and life-cycle assessment. Sustainability 2020;12(14):5666.
[20] Daniel G. Fungal degradation of wood cell walls. In: Kim S, Funada R, Singh AP, editors. Secondary xylem biology. Academic Press; 2016. p. 131–67.
[21] Worrall JJ, Anagnost SE, Zabel RA. Comparison of wood decay among diverse lignicolous fungi. Mycologia 1997;89:199–219.
[22] Takahashi T, Sakurai T. The relationship between span-depth ratio and bending characters of wood beam. Bull Shimane Agric Coll 1967;15(A-2):34–40. http://ir.lib.shimane-u.ac.jp/3904.
[23] Newlin JA, Trayer GW. Deflection of beams with special reference to shear deformations: The influence of the form of a wooden beam on its stiffness and strength-I. Natl Advis Comm Aeronaut Rep 1924;180:1–19.
[24] Yoshizawa N, Kawakami H, Sunagawa M, Yokokawa S, Idei T. Enzymatic and histochemical study of wood degradation by white-rot fungi. Bull Utsunomiya Univ For 1990;26:19–34.
[25] Messner K, Stachelberger H. Transmission electron microscope observations of white rot caused by *Trametes hirsuta* with respect to osmiophilic particles. Trans Br Mycol Soc 1984;83:209–16.
[26] Sugai-Guérios MH, Balmant W, Krieger N, Furigo Junior A, Mitchell DA. More random-walk than autotropism: A model-based study on how aerial hyphae of Rhizopus oligosporus grow in solid-state fermentation. Biochem Eng J 2019;141:49–59.
[27] García-Segovia P, Andrés-Bello A, Martínez-Monzó J. Rehydration of air-dried Shiitake mushroom (Lentinus edodes) caps: Comparison of conventional and vacuum water immersion processes. LWT - Food Sci Technol 2011;44:480–8.
[28] Wessels JGH. Hydrophobins: proteins that change the nature of the fungal surface. Advances in microbial physiology. In: Poole RK, editor. Advances in microbial physiology, vol. 38. Academic Press; 1996. p. 1–45.
[29] Sun W, Tajvidi M, Hunt CG, Howell C. All-natural smart mycelium surface with tunable wettability. ACS Appl Bio Mater 2021;4:1015–22.
[30] Hakkou M, Petrissans M, Zoulalian A, Gerardin P. Investigation of wood wettability changes during heat treatment on the basis of chemical analysis. Polym Degrad Stab 2005;89:1–5.
[31] Rahardjo YSP, Weber FJ, Paul Le Comte E, Tramper J, Rinzema A. Contribution of aerial hyphae of Aspergillus oryzae to respiration in a model solid-state fermentation system. Biotechnol Bioeng 2002;78:539–44.
[32] Sun W, Tajvidi M, Howell C, Hunt CG. Functionality of surface mycelium interfaces in wood bonding. ACS Appl Mater Interfaces 2020;12:57431–40.
[33] Saleem Q, Wildman RD, Huntley JM, Whitworth MB. Material properties of semi-sweet biscuits for finite element modelling of biscuit cracking. J Food Eng 2005;68:19–32.
[34] Jones M, Mautner A, Luenco S, Bismarck A, John S. Engineered mycelium composite construction materials from fungal biorefineries: A critical review. Mater Des 2020;187:108397.